

BAR DISSOLUTION IN PROLATE HALOS

MAKOTO IDETA

Department of Astronomy, Kyoto University, Kyoto 606-8502, Japan; ideta@kusastro.kyoto-u.ac.jp

AND

SHUNSUKE HOZUMI

Faculty of Education, Shiga University, 2-5-1 Hiratsu, Otsu, Shiga 520-0862, Japan; hozumi@sue.shiga-u.ac.jp

Accepted for publication in ApJ Letters

ABSTRACT

The time evolution of barred structures is examined under the influence of the external forces exerted by a spherical halo and by prolate halos. In particular, galaxy disks are placed in the plane including the major axis of prolate halos, whose configuration is often found in cosmological simulations. N -body disks in fixed external halo fields are simulated, so that bars are formed via dynamical instability. In the subsequent evolution, the bars in prolate halos dissolve gradually with time, while the bar pattern in a spherical halo remains almost unchanged to the end of the simulation. The decay times of the bars suggest that they can be destroyed in a time smaller than a Hubble time. Our results indicate that this dissolution process could occur in real barred galaxies, if they are surrounded by massive dark prolate halos, and the configuration adopted here is not unusual from the viewpoint of galaxy formation. For a prolate halo model, an additional simulation that is restricted to two-dimensional in-plane motions has also ended up with similar bar dissolution. This means that the vertical motions of disk stars do not play an essential role in the bar dissolution demonstrated here.

Subject headings: galaxies: evolution — galaxies: halos — galaxies: kinematics and dynamics — galaxies: structure — methods: n -body simulations

1. INTRODUCTION

Observations of disk galaxies have shown that their rotation curves are often flat out to large distances (e.g., Rubin et al. 1982, 1985; Kent 1987). This finding suggests that disk galaxies, regardless of whether they are barred or non-barred, are surrounded by massive dark halo. However, it is difficult to distinguish between barred and non-barred galaxies from edge-on views which can easily provide rotation curve data. Recent development of observations enables us to measure rotation curves of barred galaxies, even though they are not viewed fully edge-on. As a result, it has been confirmed that many, if not all, barred galaxies show flat rotation curve, which does suggest the existence of massive dark halo in barred galaxies as well (Kormendy 1983; Peters et al. 1994).

The shape of dark matter halo, on the other hand, remains uncertain observationally, although some indication is obtained (Sackett 1999). Cosmological simulations demonstrate that dark matter halos are inclined to be more frequently prolate than oblate (Dubinski & Carlberg 1991; Warren et al. 1992). In addition, prolate halos can be supported from the standpoint of the longevity of galactic warps; I detta et al. (2000) have shown that a warped structure persists for a long time in a prolate halo while it disappears quickly in an oblate halo.

Recently, El-Zant & Haßler (1998) have revealed that bars are likely to be destroyed owing to chaotic diffusion of bar-supporting orbits, if they are embedded in triaxial halos including prolate configurations. Their results indicate that such bar destruction is conceivable from the situation where a barred galaxy is placed in a prolate halo with the major axis of the halo being in the disk plane. Ac-

cording to Warren et al.'s (1992) cosmological simulations, this configuration of a disk in a prolate-like halo often occurs. Thus, real barred galaxies might be surrounded by prolate halos, and could suffer forces caused by the elongated potential of those halos. Unfortunately, however, El-Zant & Haßler (1998) treated all the components of a bar, disk and halo as fixed potentials, and analyzed the orbits of test stars. Consequently, it is unclear whether bars are in reality destroyed in such prolate halos.

In this *Letter*, we demonstrate from N -body simulation that a barred structure is, in fact, completely destroyed in a time smaller than a Hubble time if it is embedded in a prolate halo whose major axis is placed in the disk plane. In §2, we describe the initial setup of our models and the numerical method. Results are presented in §3. A discussion and conclusions are given in §4.

2. MODELS AND METHOD

We set up a configuration such that the mid-plane of a galaxy disk is put in the plane including the major axis of a prolate halo. For comparison, a spherical halo is also included in our models. As a first step, the halo is handled as a fixed external field. We will discuss the possible effects of a live halo on the evolution of a bar pattern in the last section. The disk is evolved forward in time to form a bar via dynamical instability. Thereafter, we examine how the barred structure is influenced in the prolate halo. Since we pay attention to mainly the effects of an elongated halo on a bar, we do not include a bulge component which acts to reduce the amplitudes of the bars arising from the bar instability (Hozumi, Fujiwara, & Nishida 1987).

The prolate halo models are constructed from an axisymmetric modification of Hernquist's models (Hernquist

1990). The density profile of the halos is represented by

$$\rho_h(m) = \frac{M_h}{2\pi a c^2} \frac{1}{m(1+m)^3}, \quad (1)$$

where M_h is the halo mass, a and c are the scale lengths along the major and minor axes, respectively, and

$$m^2 = \frac{x^2}{a^2} + \frac{y^2 + z^2}{c^2}. \quad (2)$$

If the ratio of c to a is smaller than unity, the halo is prolate. We choose $c/a = 0.6$ and 0.75 as prolate halos, and $c/a = 1$ as a spherical halo. The models with $c/a = 0.6, 0.75$, and 1 are named Models P060, P075, and S100, respectively.

We adopt an exponential surface-density profile (Freeman 1970) with an isothermal density distribution in the vertical direction (Spitzer 1942) for the disk models that are given by

$$\rho_d(R, z) = \frac{M_d}{4\pi R_d^2 z_d} \exp\left(-\frac{R}{R_d}\right) \operatorname{sech}^2\left(\frac{z}{z_d}\right), \quad (3)$$

where M_d is the disk mass, R_d is the scale length, and z_d is the scale height. The disks are truncated radially at $15 R_d$, and vertically at $2 z_d$. The velocity distribution of disk particles is realized by employing Hernquist's (1993) approach which is based on the moments of the collisionless Boltzmann equation. In setting up the particle velocities, the disk plane is placed to include the major axis of the prolate halo. The typical Toomre Q parameter (Toomre 1964) is chosen to be of order unity so as to induce the bar instability easily, and the value, $Q = 1$, is set at the radius corresponding to the sun in the physical units of the Galaxy described below.

TABLE 1
PARAMETERS FOR N -BODY SIMULATIONS

Model	M_d	R_d	z_d	M_h	a	c
P060.....	1.0	1.0	0.2	9.0	10.0	6.0
P075.....	1.0	1.0	0.2	9.0	10.0	7.5
S100.....	1.0	1.0	0.2	9.0	10.0	10.0

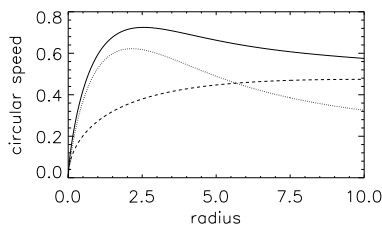


FIG. 1.— Circular speed showing the contribution from the halo (dashed line) and disk (dotted line) to the total (solid line) for Model S100.

We employ a system of units such that the gravitational constant $G = 1$, the disk mass $M_d = 1$, and the scale length $R_d = 1$. If these units are scaled to physical values appropriate for the Milky Way, i.e., $R_d = 3.5$ kpc and $M_d = 5.6 \times 10^{10} M_\odot$, unit time and velocity are 1.31×10^7 yr and 262 km s $^{-1}$, respectively. The scale height z_d is set to be 0.2 , or in our units, 700 pc, which corresponds to that of old stars in the Milky Way. The disk is

represented by 100,000 particles of equal mass. Since flat rotation curves of spiral galaxies suggest that the mean halo-to-disk mass ratio at the Holmberg radius is 1.0 (e.g., Carignan & Freeman 1985), we determine the halo mass so that the disk and halo masses within $5 R_d$ are equal to each other in the spherical halo model. The parameters of each model are presented in Table 1, and the rotation curve of Model S100 is shown in Figure 1.

We use a hierarchical tree algorithm (Barnes & Hut 1986) with an opening angle criterion, $\theta = 0.75$, being adopted. We expand forces and potentials up to quadrupole terms in the tree code. Forces are softened with a cubic spline (Hernquist & Katz 1989), and the spline softening length is $0.04 R_d$, or in other words, $0.2 z_d$. The equations of motion are integrated with a fixed timestep, $\Delta t = 0.04$, using a leapfrog method. For these choices of parameters, the total energy was conserved to better than 0.13% in all simulations.

3. RESULTS

Figure 2 shows the contour plots of face-on density profiles at intervals of 120 time units for Models P060, P075, and S100. In all the models, bars were formed through the bar instability, and they were almost fully developed by $t \simeq 120$. We can see from Figure 2 that in the subsequent evolution, the bar pattern was kept nearly unchanged to the end of the simulation for the spherical halo model (Model S100), while the bars continued to dissolve gradually with time for the prolate halo models (Models P060 and P075). To evaluate the change in bar shape, we derived the axis ratio of the bars from the moment of inertia tensor for disk particles included in $2.0 R_d$ at which the bars end roughly. Then, we have found that the axis ratio changed from $\simeq 0.71$ at $t = 150$ to $\gtrsim 0.95$ at $t = 600$ for Model P060, and that it did from $\simeq 0.68$ at $t = 150$ to $\gtrsim 0.93$ at $t = 600$ for Model P075.

To quantify the deformation of the bars formed in each halo model, we calculated their amplitudes as follows. The bars are very thin as compared to the extent of the disks, so that we ignore the thickness of the bars by projecting the particle distributions to the mid-plane of the disks. Then, we expand the density and potential of the projected distribution in a set of basis functions as

$$\mu(\mathbf{R}) = \sum_{n,m} A_{nm} \mu_{nm}(\mathbf{R}), \quad (4)$$

$$\Phi(\mathbf{R}) = \sum_{n,m} A_{nm} \Phi_{nm}(\mathbf{R}), \quad (5)$$

where each density-potential pair, μ_{nm} and Φ_{nm} , constitutes Aoki & Iye's (1978) basis set given by

$$\mu_{nm}(\mathbf{R}) = \frac{2n+1}{2\pi} \left(\frac{1-\xi}{2}\right)^{3/2} P_{nm}(\xi) \exp(im\theta), \quad (6)$$

$$\Phi_{nm}(\mathbf{R}) = -\left(\frac{1-\xi}{2}\right)^{1/2} P_{nm}(\xi) \exp(im\theta). \quad (7)$$

Here, P_{nm} are the Legendre functions ($n \geq m$), and the radial transformation

$$\xi = \frac{R^2 - 1}{R^2 + 1} \quad (8)$$

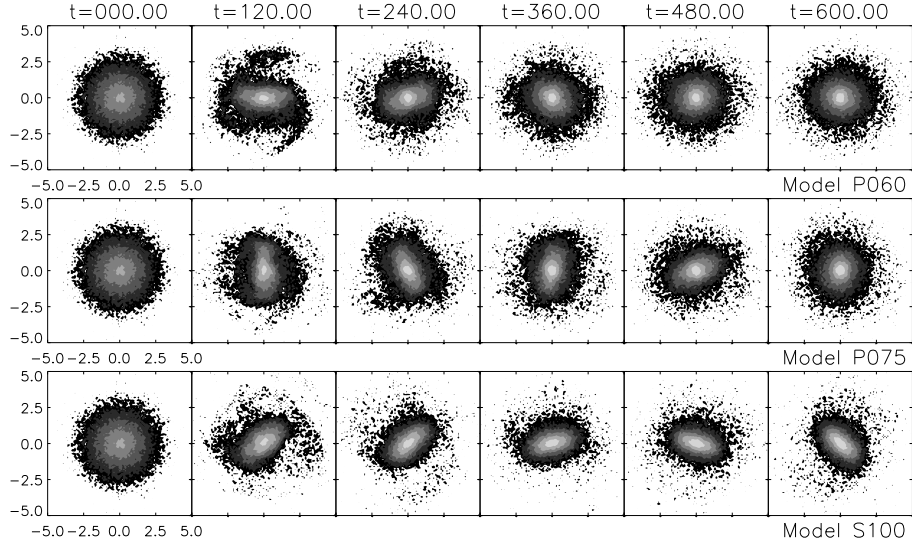


FIG. 2.— Time evolution of the face-on density contours for Models P060 (top row), P075 (middle row), and S100 (bottom row). In all the models, bars are almost fully developed by $t=120$. The bar in the spherical halo model (Model S100) continues to exist to the end of the simulation, while the bars in the prolate halo models (Models P060 and P075) are weakened gradually with time and are completely destroyed at the end.

is used. Positive values of m correspond to the number of arms in spiral patterns. In the expansions shown above, the amplitude of the (n, m) -mode is calculated from the absolute value of the expansion coefficient, $|A_{nm}|$. In particular, we pay attention to the fastest growing bar mode with $(n, m) = (2, 2)$.

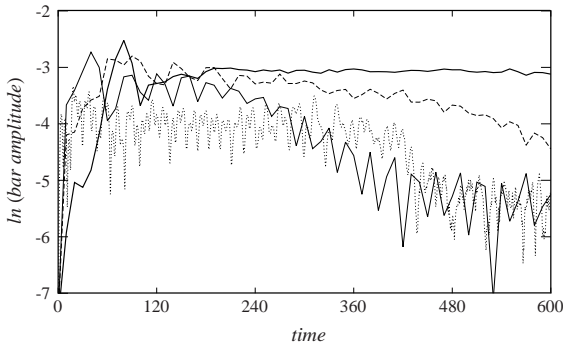


FIG. 3.— Time evolution of the bar amplitude of the fastest growing mode for Models P060 (thin solid line), P075 (dashed line), and S100 (thick solid line). Also shown is the time evolution of the bar amplitude for a two-dimensional analogue of Model P060 (dotted line).

In Figure 3, we present the time evolution of the bar amplitude, $|A_{22}|$, for each halo model. This figure describes the behavior of the barred structures seen in Figure 2 quantitatively. Again, we find that the bars have grown up to their full amplitudes by $t \simeq 120$. In particular, it should be emphasized that the bar amplitude decays nearly exponentially with time $\sim \exp(-t/\tau)$ for the prolate halo models while it remains practically constant to the end of the simulation for the spherical halo model. To estimate the decay times τ , least-squares fits were applied to the data from $t = 200$ to $t = 400$ for Model P060, and to those from $t = 200$ to 600 for Model P075. We obtained $\tau \simeq 111$ and $\tau \simeq 375$ for Models P060 and P075, respectively. If these values are represented by the physical

units appropriate for the Milky Way, the decay times correspond to $\sim 1.5 \times 10^9$ yr and $\sim 4.9 \times 10^9$ yr, respectively. These time intervals are relatively smaller than a Hubble time that is almost equivalent to the supposed ages of disk galaxies, even though it takes about twice as long as the decay times for the bar amplitude to decrease by an order of magnitude. Thus, this kind of bar dissolution addressed here could occur in real barred galaxies, provided that our models reflect physical realism to a reasonable degree.

4. DISCUSSION AND CONCLUSIONS

We have found that a prolate halo can destroy a bar in a time smaller than a Hubble time, if the major axis of the halo lies in the disk plane. It has been known that a bar can be destructed by central massive objects (Norman, Sellwood, & Hasan 1996; Hozumi & Hernquist 1999), and also by close encounter or minor merger of nearby dwarf galaxies (Athanassoula 1996). Our finding adds another situation where bar dissolution can occur even without recourse to massive central objects or nearby companion galaxies. Thus, in considering the evolution of barred galaxies, we should take into account the shape of surrounding halos and their configurations to the disks that support the bars.

The time scale of bar dissolution will depend on the parameters of halos such as the mass, core radius, and axis ratio. Then, to investigate whether real barred galaxies can experience bar dissolution, we need to check out how realistic our models are. First, for a halo model, we have used Hernquist's models that have a density profile proportional to r^{-1} near the center. Such a central cuspy density profile might be a natural end-product of hierarchical clustering based on a standard cold dark matter scenario (e.g., Navarro, Frenk, & White 1996, 1997; Fukushige & Makino 1997). From this point of view, our adopted halo density profiles would not be peculiar. Next, the halo mass and core radius were chosen to follow the observed rotation curves in spiral galaxies such that the circular velocities

are almost constant out to large radii. Thus, the kinematic structures of the systems adopted here would not differ substantially from those of real galaxies. Last, Model P075 ($c/a = 0.75$) also leads to bar destruction within a Hubble time. Since cosmological simulations demonstrate that the angular momentum vector of galactic disks is often aligned to the minor axis of dark halos, the axis ratio of halos in the disk plane corresponds to the major-to-intermediate one. According to Figure 7a of Warren et al. (1992), the cumulative fraction of the dark halos that have a major-to-intermediate axis ratio smaller than 0.75 amounts to about 70%. In addition, the observationally determined geometrical form of dark halos is shown to be $(b/a)_\rho \gtrsim 0.8$ as the equatorial axis ratio in density, and $(c/a)_\rho = 0.5 \pm 0.2$ as the vertical-to-equatorial axis ratio in density (Sackett 1999). These values indicate that halos tend to be prolate with the major axis being in the disk plane, and that the axis ratio of $c/a = 0.75$ employed in our simulation is not far from the current lowest limit of 0.8. Taking into consideration those aspects mentioned above, bar dissolution might be in progress in the real universe.

As a possible mechanism of bar destruction, Raha et al. (1991) pointed out the bar buckling instability that is known as the firehose instability. This instability originates in the anisotropic velocity dispersion between the motions parallel to and those vertical to the disk. If this is the case for the bar destruction presented here, a bar should survive in an infinitesimally thin disk, irrespective of the surrounding halo shape. Then, we run an additional simulation in which the motions of stars are restricted to the plane of the disk with a self-consistent field (SCF) method (Clutton-Brock 1972; Hernquist & Ostriker 1992) using Aoki & Iye's basis set (eqs. [6] and [7]). The model realized with 100,000 particles of equal mass is a two-dimensional analogue of Model P060. In the SCF code, the maximum number of radial expansion coefficients is taken to be 16, and that of azimuthal ones is chosen to be 2 with only even values being used ($m = 0$, and 2). The resulting behavior of the bar amplitude defined by $|A_{22}|$ is indicated by the dotted line in Figure 3. Clearly, the bar amplitude decreases nearly exponentially with time, and its time evolution is quite similar to that in the correspond-

ing three-dimensional simulation (Model P060). This fact implies that the buckling instability should not be the essential cause of the bar destruction found in our three-dimensional simulations.

Another likely mechanism of bar destruction is the effect of chaotic orbits. Recently, El-Zant & Haßler (1998) have found that the orbits that support a bar are highly chaotic when the barred galaxy is embedded in a triaxial halo whose minor axis is vertical to the disk plane. Then, they suggest that the bar may be destroyed owing to chaotic diffusion, although they do not mention the destruction time scale. Norman et al. (1996) have revealed that a bar is destroyed within a few dynamical times after the contraction of a rigid mass component, whose mass exceeds some critical value, is completed to form a central massive object. As a result, they are led to a picture that the abrupt destruction of a bar results from the chaotic behavior of bar-supporting orbits. However, our results show the gradual erosion of bars, and so, the behavior of the bar amplitude is closer to that found by Hozumi & Hernquist (1999) who examined secular change in bar pattern caused by central massive black holes added to flat disks. Of course, chaotic orbits might lead to the gradual destruction of bars. Therefore, we will analyze our models in phase space to study stochasticity in stellar orbits in a separate paper.

Our simulations are highly idealized in that halos were treated as external fixed potentials. If halos are made mobile, the pattern speed of a bar will quickly slow down owing to dynamical friction of the halos (Weinberg 1985; Debattista & Sellwood 1998). It is conceivable that the time scale of bar destruction could be affected by the pattern speed of a bar. Thus, a wider variety of simulations with a greater degree of realism will be required to figure out the detailed processes of bar dissolution.

We are grateful to Dr. T. Tsuchiya for useful discussions. We also thank Dr. K. Ohta for helpful comments on the observational side of barred galaxies. Numerical simulations were carried out on VPP/16R and VX/4R at the Astronomical Data Analysis Center of the National Astronomical Observatory, Japan (ADAC/NAOJ).

REFERENCES

Aoki, S., & Iye, M. 1978, PASJ, 30, 519
 Athanassoula, E. 1996, in ASP Conf. Ser. 91, Barred Galaxies, ed. R. Buta, D. A. Crocker, & B. G. Elmegreen (San Francisco: ASP), 309
 Barnes, J., & Hut, P. 1986, Nature, 324, 446
 Carignan, C., & Freeman, K. C. 1985, ApJ, 294, 494
 Clutton-Brock, M. 1972, Ap&SS, 16, 101
 Debattista, V. P., & Sellwood, J. A. 1998, ApJ, 493, L5
 Dubinski, J., & Carlberg, R. G. 1991, ApJ, 378, 496
 El-Zant, A. A., & Haßler, B. 1998, NewA, 3, 493
 Freeman, K. C. 1970, ApJ, 160, 811
 Fukushige, T., & Makino, J. 1997, ApJ, 477, L9
 Hernquist, L. 1990, ApJ, 356, 359
 Hernquist, L. 1993, ApJS, 86, 389
 Hernquist, L., & Katz, N. 1989, ApJS, 70, 419
 Hernquist, L., & Ostriker, J. P. 1992, ApJ, 386, 375
 Hozumi, S., Fujiwara, T., & Nishida, M. T. 1987, PASJ, 39, 447
 Hozumi, S., & Hernquist, L. 1999, in ASP Conf. Ser. 182, Galaxy Dynamics, ed. D. Merritt, J. A. Sellwood, & M. Valluri (San Francisco: ASP), 259
 Ideta, M., Hozumi, S., Tsuchiya, T., & Takizawa, M. 2000, MNRAS, 311, 733
 Kent, S. M. 1987, AJ, 93, 816
 Kormendy, J. 1983, ApJ, 275, 529
 Navarro, J. F., Frenk, C. S., & White, S. D. M. 1996, ApJ, 462, 563
 Navarro, J. F., Frenk, C. S., & White, S. D. M. 1997, ApJ, 490, 493
 Norman, C. A., Sellwood, J. A., & Hasan, H. 1996, ApJ, 462, 114
 Peters, W. L., Freeman, K. C., Forster, J. R., Manchester, R. N., & Ables, J. G. 1994, MNRAS, 269, 1025
 Raha, N., Sellwood, J. A., James, R. A., & Kahn, F. D. 1991, Nature, 352, 411
 Rubin, V. C., Burstein, D., Ford, W. K., Jr., & Thonnard, N. 1985, ApJ, 289, 81
 Rubin, V. C., Ford, W. K., Jr., Thonnard, N., & Burstein, D. 1982, ApJ, 261, 439
 Sackett, P. D. 1999, in ASP Conf. Ser. 182, Galaxy Dynamics, ed. D. Merritt, J. A. Sellwood, & M. Valluri (San Francisco: ASP), 393
 Spitzer, L., Jr. 1942, ApJ, 95, 329
 Toomre, A. 1964, ApJ, 139, 1217
 Warren, M. S., Quinn, P. J., Salmon, J. K., & Zurek, W. H. 1992, ApJ, 399, 405
 Weinberg, M. D. 1985, MNRAS, 213, 451